Articles

Zirconocene Allyl Complexes: Dynamics in Solution, Reaction with Aluminum Alkyls, $B(C_6F_5)_3$-Induced Propene Insertion, and Density-Functional Calculations on Possible Formation and Reaction Pathways

Susanna Lieber, Marc-Heinrich Prosenc,*,† and Hans-Herbert Brintzinger*

Fakultät für Chemie, Universität Konstanz, D-78457 Konstanz, Germany

Received July 30, 1999

The complex $(C_5H_5)_2Zr(Me)(methallyl)$ (**1**) was prepared and studied as a model for Zr-bound allyl species which are likely to arise in zirconocene-based polymerization systems. **1** undergoes allyl−alkyl exchange with trimethyl aluminum (TMA) or with methyl alumoxane (MAO) at rates that are proportional to the Al concentration, but remain 1−2 orders of magnitude below those of typical olefin insertions. Its perfluorotriphenylborane adduct **2**, i.e., the contact ion pair $(C_5H_5)_2Zr(methallyl)^+H_3CB(C_6F_5)_3^-$, has been characterized with regard to the rearrangement dynamics of its allyl ligand. Propene reacts with **2**, at rates which are substantially lower again than those of cationic Zr−alkyl species, under insertion between Zr and one of the allylic termini. Scrambling of deuterium from an allylic CD_2 terminus over several C atom positions next to the unsaturated chain end indicates rather extensive metal migration within an initial olefin insertion product. Density-functional calculations indicate that insertion of propene directly into an η^3-coordinated Zr−allyl unit occurs with lower activation energy than insertion into an η^1-bound Zr−allyl species and that the lowest-energy pathway for the reactivation of a cationic zirconocene allyl species is its reconversion to the corresponding Zr−alkyl species by molecular hydrogen.

Downloaded by CARLI CONSORTIUM on June 29, 2009
Published on January 25, 2000 on http://pubs.acs.org | doi: 10.1021/om9906058

Introduction

Zirconocene-based catalysts for the polymerization of α-olefins have been widely studied with regard to the production of homo- and copolymers with variable molecular weights and degrees of tacticity.[1] While most of these catalyst systems are highly active initially, rates of monomer uptake generally decrease to rather small fractions of their initial values within a few hours or, in some cases, even within a few minutes.[2,3] At present, it is not fully understood which mechanisms cause this deactivation.

One mechanism that has been postulated in this regard is the formation of less active or inactive zirconium−allyl complexes.[4−9] The formation of lanthanocene allyl complexes as deactivated species was first observed by Schumann, Marks, and co-workers.[4] In a study on the catalyst system $(C_5Me_5)_2ZrMe(THT)^+$-$B(C_6H_5)_4^-$,[5] Teuben and co-workers noted that deuteriolysis of the deactivated catalyst, which gave a mixture of propene-d_1 and isobutene-d_1, indicated the presence of zirconocene−allyl complexes in this reaction system. In a complex of the type $(C_5Me_5)_2Zr(alkyl)(alkene)^+$ a hydrogen atom is apparently transferred from a CH_3 substituent of the coordinated alkene to the Zr-bound alkyl group, such that formation of a Zr−allyl cation is accompanied by liberation of an alkane (Scheme 1). Formation of zirconocene−allyl complexes through C−H activation of isobutene in a zirconocene−alkyl cation was also observed by Horton and by van der Heijden and Hessen.[10,11]

Alternatively, a zirconocene−alkyl cation could undergo β-H transfer to the metal and subsequent C−H activation of a CH_2R or CH_3 substituent of the resulting olefin ligand to give an allyl cation of the type $(C_5H_5)_2$-

† Present address: University of North Carolina at Chapel Hill, Venable and Kenan Laboratories, B 421 CB #3290, Chapel Hill, NC 27599-3290.

(1) Brintzinger, H. H.; Fischer, D.; Mülhaupt, R.; Rieger, B.; Waymouth, R. *Angew. Chem., Int. Ed. Engl.* **1995**, *34*, 1143. Bochmann, M. *J. Chem. Soc., Dalton Trans.* **1996**, 255. Kaminsky, W. *J. Chem. Soc., Dalton Trans.* **1998**, 1413.

(2) Fischer, D.; Mülhaupt, R. *J. Organomet. Chem.* **1991**, *417*, C7.

(3) Chien, J. C. W.; Sugimoto, R. J. *J. Polym. Sci.* **1991**, *29*, 459.

(4) Jeske, G.; Lauke, H.; Schock, L. E.; Swepstone, P. N.; Schumann, H.; Marks, T. J. *J. Am. Chem. Soc.* **1985**, *107*, 8103. Jeske, G.; Lauke, H.; Mauermann, H.; Swepstone, P. N.; Schumann, H.; Marks, T. J. *J. Am. Chem. Soc.* **1985**, *107*, 8091.

(5) Eshuis, J. J. W.; Tan, Y. Y.; Meetsma, A.; Teuben, J. H.; Renkema, J.; Evens, G. G. *Organometallics* **1992**, *11*, 362.

(6) Richardson, D. E.; Alameddin, G. N.; Ryan, M. F.; Hayes, T.; Eyler, J. R.; Siedle, A. R. *J. Am. Chem. Soc.* **1996**, *118*, 11244.

(7) Pindando, G. J.; Thornton-Pett, M.; Bouwkamp, M.; Meetsma, A.; Hessen, B.; Bochmann, M. *Angew. Chem., Int. Ed. Engl.* **1997**, *37*, 22358.

(8) Feichtinger, D.; Plattner, D. A.; Chen, P. *J. Am. Chem. Soc.* **1998**, *120*, 7125.

(9) Guyot, A.; Spitz, R.; Dassaud, J.-P.; Gomez, C. *J. Mol. Catal.* **1993**, *82*, 29.

(10) Horton, A. D. *Organometallics* **1996**, *15*, 2675.

(11) van der Heijden, H.; Hessen, B.; Orpen, A. G. *J. Am. Chem. Soc.* **1998**, *120*, 1112.

10.1021/om9906058 CCC: $19.00 © 2000 American Chemical Society
Publication on Web 01/25/2000

Scheme 1

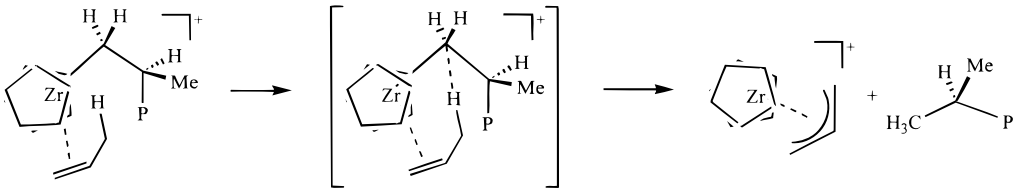

P = polymer chain

Scheme 2

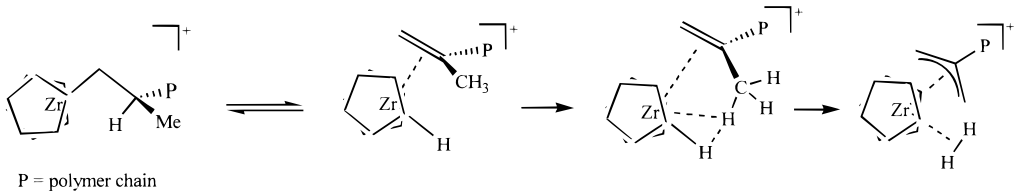

P = polymer chain

$Zr(allyl)^+$ together with dihydrogen (Scheme 2).[12] Formation of dihydrogen gas in the course of zirconocene-catalyzed olefin polymerizations was indeed observed by Horton[13] and by Karol and Wassermann[14] and proposed to be due to the formation of allyl complexes in the catalyst systems studied. Direct observations on the formation of Zr−methallyl complexes by C−H activation of isobutene under release of H_2 were obtained by Richardson and co-workers from gas-phase MS studies.[6] Recently, Resconi has discussed possible roles of zirconocene−allyl complexes in stereoerror formation by chain-end isomerizations,[15] which are observed particularly at reduced monomer concentrations.[16,17]

The further fate of any such allyl species arising during polymerization catalysis is not clear. Teuben and co-workers assumed that a $(C_5Me_5)_2Zr(allyl)^+$ complex is catalytically inactive.[5] Guyot, Spitz, and co-workers postulated that inactive Ti−allyl complexes formed by Ti-based heterogeneous catalysts might be reconverted to active Ti−alkyl species by alkyl exchange with aluminum alkyls.[9] Erker and co-workers, on the other hand, observed the insertion of α-olefins into a zirconocene allyl−borate "betain" species, derived from a Zr−butadiene complex by reaction with $B(C_6F_5)_3$.[18]

It thus remains to be explored whether—and at which rates—olefins can insert into Zr−allyl complexes which might arise in a catalytic reaction system. Here we report results of experimental and theoretical studies on possible reaction pathways of zirconocene−allyl model complexes.

Results and Discussion

The dynamic behavior of Zr−allyl complexes and their reactivity toward Lewis acids and olefins were studied using the 2-methylallyl (methallyl) zirconocene complex $(C_5H_5)_2ZrMe(C_4H_7)$, **1**, as a model for an allyl complex carrying a polymer alkyl chain. This complex was prepared and isolated by reaction of excess methallylmagnesium chloride in THF with $(C_5H_5)_2ZrMeCl$.[19] Complex **1** is an air- and water-sensitive yellow solid; it can be recrystallized from pentane in the form of small yellow needles. Complex **1** is soluble and stable in ethers and hydrocarbons but decomposes slowly in chlorinated solvents. ^1H NMR spectra of **1** in C_6D_6 at room temperature give rise to only one resonance for all four allylic protons. ^1H and ^{13}C chemical shifts of the terminal CH_2 groups of the C_4H_7 ligand, 2.54 and 67 ppm, respectively, and an IR absorption at 1520 cm^{-1} correspond to an η^3-π-bound, rather than to an η^1-σ-bound allyl group.[20] The equivalence of all terminal allyl protons even at −90 °C indicates a rapid haptotropic allyl rearrangement[21] with a low activation barrier of $\Delta G^{\ddagger} < 30$ kJ/mol.

1. Reaction with Aluminum Alkyls. To study the reactivity of complex **1** toward aluminum-based cocatalysts, 1 M solutions of trimethylaluminum (TMA) were mixed with C_6D_6 solutions of complex **1** in a glovebox. Reaction of complex **1** with 1 equiv of TMA (i.e., 0.5 equiv of Al_2Me_6) causes the bright yellow color of complex **1** to diminish. New signals appearing in the ^1H NMR spectra at 5.7 and −0.15 ppm were assigned to $(C_5H_5)_2ZrMe_2$. A new methallyl species, presumably $Me_2Al-C_4H_7$, gives rise to a broad singlet at 2.92 ppm and to a likewise broadened CH_3 signal appearing at 1.76 ppm, rather than at 2.54 and 1.5 ppm, as observed in complex **1**.

(12) A similar reaction path for ethene polymerization was studied by: Margl, P. M.; Woo, T. K.; Ziegler, T. *Organometallics* **1998**, *17*, 4997.

(13) Horton, A. D. Private communication, 1998.

(14) Karol, F. J.; Kao, S.-C.; Wassermann, E. P.; Brady, R. C. *New J. Chem.* **1997**, *21*, 797. Wassermann, E. P. *Abstracts of Papers, ACS*, 081-poly, 1998; 216.

(15) Resconi, L.; Camurati, I.; Sudmeijer, O. *Top. Catal.* **1999**, *7*, 145.

(16) Busico, V.; Cipullo, R. *J. Am. Chem. Soc.* **1994**, *116*, 9329.

(17) (a) Leclerc, M. K.; Brintzinger, H. H. *J. Am. Chem. Soc.* **1995**, *117*, 1651. (b) Leclerc, M. K.; Brintzinger, H. H. *J. Am. Chem. Soc.* **1996**, *118*, 9024. (c) Prosenc, M. H.; Brintzinger, H. H. *Organometallics* **1997**, *16*, 3889.

(18) Insertion of one propene/Zr into the "betaine" complex $(C_5H_5)_2$-$Zr(\eta^3$-$CH_2CHCH_2CH_2B(C_6F_5)_3)$ was reported by Erker and co-workers: Temme, B.; Karl, J.; Erker, G. *Chem. Eur. J.* **1996**, *2*, 919. Karl, J.; Erker, G.; Fröhlich, R. *J. Am. Chem. Soc.* **1997**, *119*, 11165. Karl, J.; Erker, G. *J. Mol. Catal.* **1998**, *128*, 85.

(19) Wailes, P. C.; Weigold, H.; Bell, A. P. *J. Organomet. Chem.* **1971**, *33*, 181.

(20) Martin, H. A.; Lemaire, P. J.; Jellinek, F. *J. Organomet. Chem.* **1968**, *14*, 149. Schlosser, M.; Stähle, M. *Angew. Chem.* **1980**, *92*, 497. Wilke, G.; Bogdanovic, B.; Hardt, P.; Heimbach, P.; Keim, W.; Kröner, M.; Oberkirch, W.; Tanaka, K.; Steinrücke, E.; Walter, D.; Zimmermann, H. *Angew. Chem.* **1966**, *78*, 157.

(21) Krieger, J. K.; Deutch, J. M.; Whitesides, G. M. *Inorg. Chem.* **1973**, *12*, 1535. Erker, G.; Berg, K.; Angermund, K.; Krüger, C. *Organometallics* **1987**, *6*, 2620. Landis, C. R.; Cleveland, T.; Casey, C. P. *Inorg. Chem.* **1995**, *34*, 1285; Abrahams, M. B.; Yoder, J. C.; Loeber. C.; Day, M. W.; Bercaw, J. E. *Organometallics* **1999**, *18*, 1873.

Downloaded by CARLI CONSORTIUM on June 29, 2009
Published on January 25, 2000 on http://pubs.acs.org | doi: 10.1021/om9906058

Scheme 3

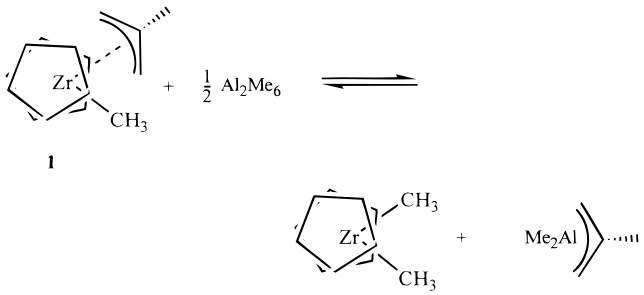

1

Table 1. Relative Concentrations of Complex 1 and $(C_5H_5)_2ZrMe_2$ and Equilibrium and Rate Constants for Their Interconversion with Respect to the Zr/Al Ratio[a]

	R_{Al} = [Zr]/[Al]			
	1:1	1:3	1:5	1:10
R_{int} = [1]/[$(C_5H_5)_2ZrMe_2$][b]	1.95	1.38	1.0	0.71
equilibrium constant[c] K_{ex}/(mol/L)$^{1/2}$	0.07	0.06	0.07	0.08
exchange rate[d] k_{obs}/s^{-1}	0.12	0.22	0.30	0.42
rate constant[e] $k_{ex}/10^3$ (mol/L)$^{-1}$ s^{-1}	1.7	1.8	1.8	1.8

[a] At a total zirconocene concentration of 0.08 mol/L in C_6D_6 solution at 300 K. [b] Integral ratio of the C_5H_5 signals of complexes **1** and $(C_5H_5)_2ZrMe_2$. [c] According to Scheme 3. [d] Determined by ^{1}H-NOESY spectra according to ref 22. [e] Derived from $k_{ex} = k_{obs} \times 2([Al_2Me_6]K_{diss})^{-1/2}$ with $K_{diss} = 2.6 \times 10^{-8}$ mol/L (cf. ref 23).

This reaction between complex **1** and TMA occurred instantaneously at room temperature but did not go to completion. The final ratio between **1** and $(C_5H_5)_2ZrMe_2$ was ca. 2:1, while reaction with 1.5 equiv of Al_2Me_6 gave **1** and $(C_5H_5)_2ZrMe_2$ in a ratio of 1.4:1. For the equilibrium between these two compounds and excess Al_2Me_6 (cf. Scheme 3), the equilibrium constant K_{ex} and apparent exchange rates k_{obs} were determined in C_6D_6 solutions containing complex **1** and Al_2Me_6 in Zr:Al ratios of 1:1, 1:3, 1:5, and 1:10, using two-dimensional NMR techniques (cf. Table 1).

^{1}H-NOESY spectra of these solutions indicate methallyl−methyl exchange between the Zr centers of $(C_5H_5)_2ZrMe(C_4H_7)$ and $(C_5H_5)_2ZrMe_2$ and the Al centers of TMA and the aluminum methallyl product. Methyl−methallyl exchange between $(C_5H_5)_2ZrMe(C_4H_7)$ and $(C_5H_5)_2ZrMe_2$ is entirely suppressed in the absence of TMA. Rather than between $(C_5H_5)_2ZrMe(C_4H_7)$ and $(C_5H_5)_2ZrMe_2$ directly, the exchange thus proceeds via reversible exchange of methallyl and methyl ligands between Zr and Al centers. The apparent exchange rate constant k_{obs} is approximately proportional to the square root of the Al_2Me_6 concentration (cf. Table 1). This indicates that reaction of monomeric $AlMe_3$ with complex **1** is rate determining for the exchange process. Using an equilibrium constant $K_{diss} = 2.6 \times 10^{-8}$ mol/L for the dissociation of Al_2Me_6 to monomeric $AlMe_3$, [23] a value of $k_{ex} = 1.7 \times 10^3$ L·mol^{-1}·s^{-1} is determined for the second-order rate constant of the exchange reaction between $AlMe_3$ and complex **1** (cf. Table 1).

When this rate constant for methyl exchange between complex **1** and $AlMe_3$ is determined at varying temperatures in the range 0−40 °C, estimates of $\Delta H^{\ddagger} = +34 \pm 1$ kJ/mol and of $\Delta S^{\ddagger} = -70 \pm 2$ J/(mol·K) are obtained. The negative activation entropy is in accord with an associative process, i.e., with an attack of $AlMe_3$ at the Zr-bound methallyl ligand.

Reaction of complex **1** with TMA-free MAO[24] results in the formation of $(C_5H_5)_2ZrMe_2$ and of a species with a very broad resonance at ca. 3.1 ppm, presumably some MAO−methallyl complex. At Zr:Al ratios of ca. 1:1, 1:2, 1:5, and 1:10, we observe **1** and $(C_5H_5)_2ZrMe_2$ in ratios of 1.5:1, 1.2:1, 0.8:1, and 0.6:1, respectively. This indicates that the equilibrium between complex **1** and $(C_5H_5)_2ZrMe_2$ is established also in the presence of MAO and that the equilibrium lies somewhat farther on the side of $(C_5H_5)_2ZrMe_2$ and MAO−(C_4H_7), with an equilibrium constant $K = 0.1$ (mol/L)$^{1/2}$. 2D-NOESY data for the methyl exchange at a Zr:Al ratio of 1:10 give a lower limit of $k_{obs} = 0.4$ s^{-1},[25] which is comparable to that observed for $(C_5H_5)_2ZrMe(C_4H_7)$ and TMA.

In further experiments, complex **1** was equilibrated with 10 equiv of TMA and 1 equiv of a variety of zirconocene dimethyl complexes. In the presence of $(C_5H_4Me)_2ZrMe_2$, $(C_5H_4Me)_2ZrMe(C_4H_7)$ and $(C_5H_5)_2ZrMe(C_4H_7)$ are formed in a ratio of 1:8. This indicates that substitution of the C_5-ring disfavors the formation of an allyl complex. In accord with this, no allyl exchange was detectable when $(C_5H_5)_2ZrMe(C_4H_7)$ was analogously reacted with the more highly substituted complexes Me_2Si(2-Me-4-^{t}Bu-$C_5H_2)_2ZrMe_2$ or Me_2Si(2-Me-indenyl)$_2ZrMe_2$. In the presence of the more open complexes $Me_4C_2(C_5H_4)_2ZrMe_2$, $Me_2Si(C_5H_4)_2ZrMe_2$, or $Ph_2C(C_5H_4)$(fluorenyl)$ZrMe_2$, on the other hand, the respective methallyl complexes were found to dominate in the equilibrium mixtures, in ratios of 4:1 to 6:1 relative to $(C_5H_5)_2ZrMe(C_4H_7)$, documenting again the sensitivity of these allyl exchange equilibria with respect to steric factors. All of these exchange reactions occur only in the presence of TMA, as did those described above for $(C_5H_5)_2ZrMe_2$ and $(C_5H_5)_2ZrMe(C_4H_7)$ alone.

2. Reactions of Complex 1 with $B(C_6F_5)_3$. Upon addition of a slight excess (1.1 equiv) of tris(pentafluorophenyl) borane, the color of a solution of complex **1** in benzene changes from yellow to orange-red.[26] This is accompanied by a broadening of the singlet of the allylic protons as well as a chemical shift of the Zr-bound CH_3 group to −0.3 ppm. A chemical shift difference between the *m*- and *p*-fluorine atoms of $\Delta\delta = 3$ ppm indicates the presence of a weakly bound methylborate anion in an ion pair such as **2** (Scheme 4), which has been observed before by Horton in a study of β-methyl elimination from zirconocene neopentyl complexes.[10] Tris(pentafluorophenyl)borane thus attacks $(C_5H_5)_2ZrMe(C_4H_7)$ at its methyl group rather than at its allyl group, to yield a zirconocene−allyl cation with a coordinated methylborate group, in contrast with the reaction of TMA or MAO with $(C_5H_5)_2ZrMe(C_4H_7)$, which led to exchange of the methallyl moiety.

At temperatures below −10 °C in toluene solution, two singlets are observed for the allylic protons of complex **2**. Coalescence of these signals at 0 °C indicates

(22) Perrin, C. L.; Dwyer, T. J. *Chem. Rev.* **1990**, *90*, 935.
(23) Smith, M. B. *J. Organomet. Chem.* **1972**, *46*, 31.
(24) Tritto, I.; Donetti, R.; Sacchi, M. C.; Locatelli, P.; Zannoni, G. *Macromolecules* **1997**, *30*, 1247.
(25) Exchange between $(C_5H_5)_2ZrMe(C_4H_7)$ and MAO is accompanied by reaction of $(C_5H_5)_2ZrMe_2$ with MAO under formation of an oily precipitate, presumably $(C_5H_5)_2ZrMe^+MeMAO^-$.
(26) At zirconocene concentrations above 1 mmol/L, a red oil precipitates shortly after.

Downloaded by CARLI CONSORTIUM on June 29, 2009
Published on January 25, 2000 on http://pubs.acs.org | doi: 10.1021/om9906058

Scheme 4

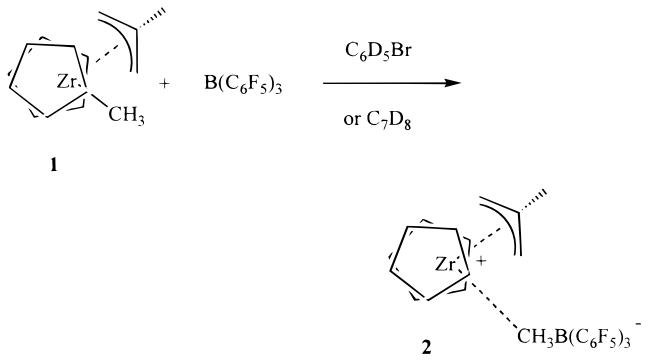

Scheme 5

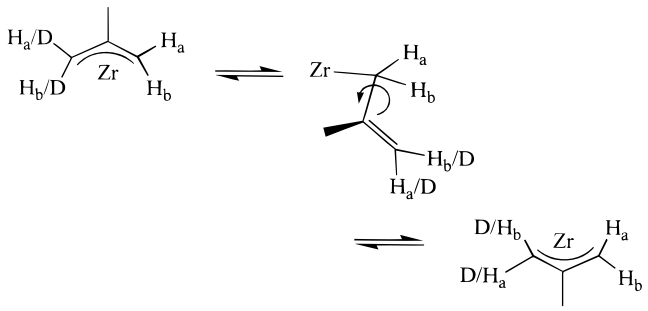

a free energy of activation of $\Delta G^{\ddagger} = 54$ kJ/mol for the haptotropic allyl rearrangement, as compared to $\Delta G^{\ddagger} < 30$ kJ/mol in complex **1.** This increased activation barrier undoubtedly arises from an increased electron deficiency at the Zr center in the ion pair **2**, which disfavors the η^1-coordination of the allyl ligand required for the exchange process.

When measured at −20 °C in bromobenzene, in which it is soluble up to 50 mmol/L, complex **2** gives rise to two separate C_5H_5 signals at 5.43 and 5.31 ppm and two sharp CH_2 signals at 2.97 and 2.45 ppm. Upon warming, the C_5H_5 signals coalesce at 5 °C, indicating a relatively facile rotation of the methallyl ligand. Coalescence of the methallyl CH_2 signals, on the other hand, requires warming to 38 °C, from which we estimate an allyl rearrangement barrier of $\Delta G^{\ddagger} = 63$ kJ/mol as compared to $\Delta G^{\ddagger} = 54$ kJ/mol in toluene. The more polar solvent appears to cause an increased charge separation in the ion pair **2** and, hence, an even stronger preference for η^3-coordination of the allyl ligand.

Determination of the exchange rates by two-dimensional ^{1}H NMR methods in the temperature range −20 to +25 °C gives activation parameters of $\Delta H^{\ddagger} = +42 \pm 1$ kJ/mol and $\Delta S^{\ddagger} = -67 \pm 4$ J/(mol·K) for the allyl rotation and of $\Delta H^{\ddagger} = +50 \pm 4$ kJ/mol and $\Delta S^{\ddagger} = -56 \pm 5$ J/(mol·K) for the haptotropic allyl rearrangement.

Isotope effects on the kinetics of this rearrangement were studied with the methylborate ion pair derived from the deuterated methallyl complex $(C_5H_5)_2ZrMe(CH_2C(CH_3)CD_2)$ (**3**). Two-dimensional ^{1}H NMR measurements in bromobenzene solution at 25 °C gave an exchange rate constant of $k_D = 22.3$ s^{-1} for the protons at the CH_2 terminus, whereas for the fully protonated complex $k_H = 16.0$ s^{-1} was obtained for the same process. The inverse kinetic isotope effect of $k_H/k_D = 0.72$ documents that the frequencies of the C−H and C−D bonds at the allylic termini increase in the exchange transition state. This is indeed to be expected if the η^3-bound allyl ligand is converted to an η^1-geometry (cf. Scheme 5), since typical IR frequencies of $\nu_{CH} = 3100$ cm^{-1} and $\nu_{CD} = 2250$ cm^{-1}, observed for CH_2 and CD_2 termini in uncomplexed α-olefins,[27] are higher than those of $\nu_{CH} = 2922$ cm^{-1} and $\nu_{CD} = 2081$ cm^{-1} observed in complex **3**.[28,29]

Attempts to generate cations with less strongly bound anions by reaction of complex **1** with *N*,*N*-dimethylanilinium tetrakis(pentafluorophenyl)borate or $[Ph_3C]^+[B(C_6F_5)_4]^-$ were not successful. *N*,*N*-Dimethylanilinium cation protonates both the methyl group and the allyl group, as indicated by evolution of isobutene.[30] When the complex $(C_5H_5)_2Zr(C_4H_7)_2$[20] was reacted with the *N*,*N*-dimethylanilinium salt, only one allyl group was protonated, but the dimethylaniline produced is partially coordinated to the Zr center, as documented by proton NMR spectra.[31]

3. Reaction of Ion Pair 2 with Propene. Upon addition of 1 equiv of propene to a solution of complex **1** and borane at −60 °C, we observe formation of short oligomeric chains, with large parts of ion pair **2** remaining unreacted, rather than insertion of one propene molecule per Zr center. At room temperature, oligomers are formed upon addition of ethene or propene. After reaction of 10−12 equiv of propene, some unreacted **2** is still detectable by NMR. These observations indicate that the first propene insertion into the Zr−allyl cation of ion pair **2** occurs significantly slower than subsequent insertions into the ensuing cationic polymeryl species.

In a sample prepared with a limited (ca. 50-fold) excess of propene, the oligomers obtained show only 2-propenyl and *n*-propyl end groups. The absence of any detectable fraction of isopropyl end groups indicates that propene inserts only into the Zr−methallyl bond of complex **2** and not into its Zr−CH_3 bond. In an effort to clarify the reaction mechanism of this insertion, in particular whether propene undergoes a (presumably α-agostically assisted) insertion into the Zr−C σ-bond of an η^1-coordinated allyl ligand[4,18] or an insertion directly into the η^3-coordinated Zr−allyl fragment (Scheme 6), we have studied the distribution of D atoms in the end groups of propene oligomers arising from the deuterated allyl complex $(C_5H_5)_2ZrMe(CH_2C(CH_3)CD_2)$ in the presence of $B(C_6F_5)_3$ and a 10−12-fold excess of propene.

In-situ D-NMR spectra of the oligomers formed in these reaction systems showed, to our surprise, substantial D-atom contents not only in the terminal and penultimate methylene groups of the oligomers, which derive from the deuterated allyl ligand, but also in methylene groups inside the oligomer chains and especially in their methyl substituents (Figure 1).[32] This

(27) Willi, A. V. *Isotopeneffekte bei chemischen Reaktionen*; G. Thieme: Stuttgart, 1983; p 20.

(28) This excludes stabilization of the η^1-coordinated intermediate by an agostic interaction of the released CD_2 terminus with the zirconium center, for which a normal kinetic isotope effect of $k_H/k_D \approx 1.3$ is expected.

(29) Prosenc, M. H.; Janiak, C.; Brintzinger, H. H. *Organometallics* **1992**, *11*, 4036.

(30) Similar observations were made by Hessen and van Hejden in studies with related Hf complexes: Hessen, B.; van Hejden, H. *J. Organomet. Chem.* **1997**, *534*, 237.

(31) Horton, A. D.; Orpen, A. G. *Organometallics* **1992**, *11*, 8.

Downloaded by CARLI CONSORTIUM on June 29, 2009
Published on January 25, 2000 on http://pubs.acs.org | doi: 10.1021/om9906058

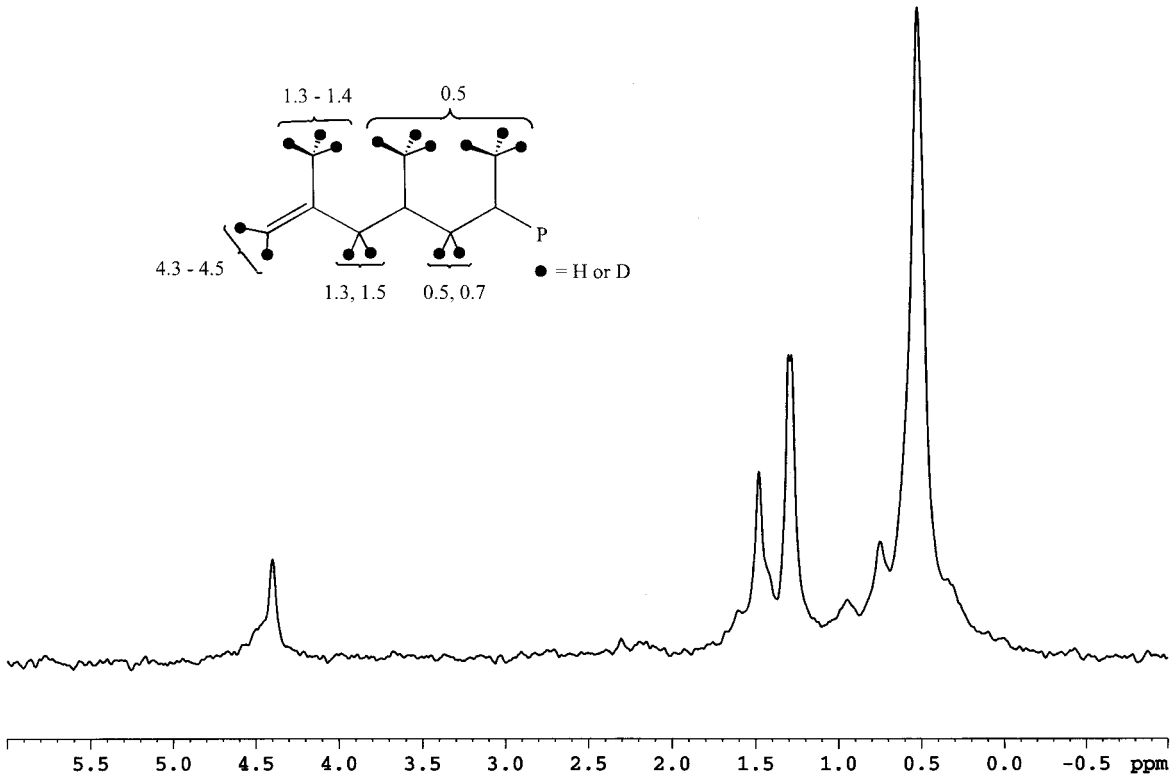

Figure 1. ^{2}H NMR spectrum of the reaction product of $[(C_5H_5)_2Zr(C_4H_5D_2)][MeB(C_6F_5)_3]$ (**4**) with 10−12 equiv of propene.

Scheme 6

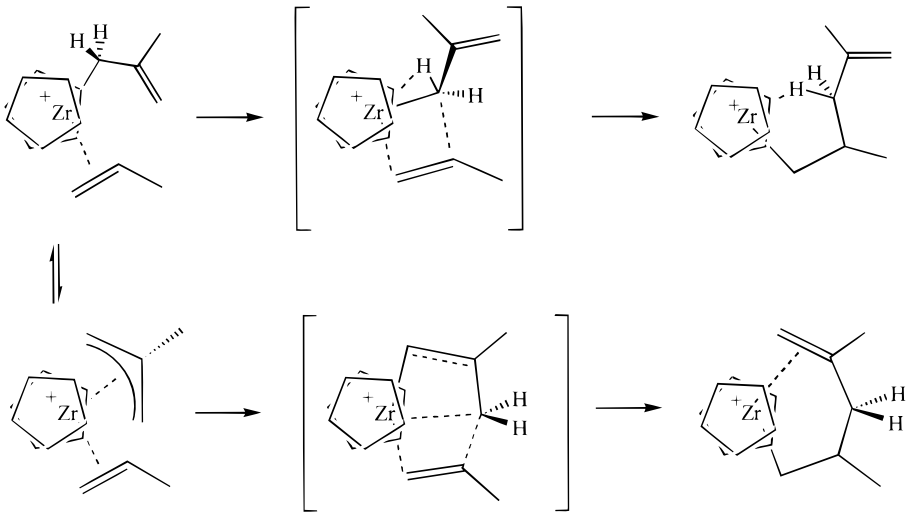

observation indicates that D atoms are efficiently scrambled between all positions of the methallyl end group and at least one adjacent propene unit. Due to this D-atom scrambling, we are not able to distinguish between insertions into an η^1-σ- and an η^3-π-bound allyl ligand. If the reaction is quenched with water immediately (within 5 s) after the addition of propene, we find substantial D-atom scrambling already; the degree of scrambling increases, however, when the reaction mixtures are kept for several hours without quenching. At present it is not clear, therefore, to which degree this D-atom scrambling occurs during the catalysis itself — i.e., concomitantly with the initial insertion steps—or by subsequent exposure of the olefinic oligomers to the Lewis-acidic reaction system.

If zirconocene catalyst centers are indeed involved, this rearrangement would probably be due to the availability of five- and six-membered cyclic intermediates (cf. Scheme 7), which allow Zr centers to migrate to either one of the adjacent methylene and methyl C atoms in a manner reminescent of the D-label scrambling between methylene and methyl groups associated with stereoerror formation by chain-end isomerizations.[16,17]

(32) In ^{13}C NMR spectra of the oligomers, a multitude of unassignable signals are apparent, presumably due to the presence of widely varying degrees of oligomerization and stereoregularity. Changes observed in the spectra of the deuterated products were thus not assignable either.

Downloaded by CARLI CONSORTIUM on June 29, 2009
Published on January 25, 2000 on http://pubs.acs.org | doi: 10.1021/om9906058

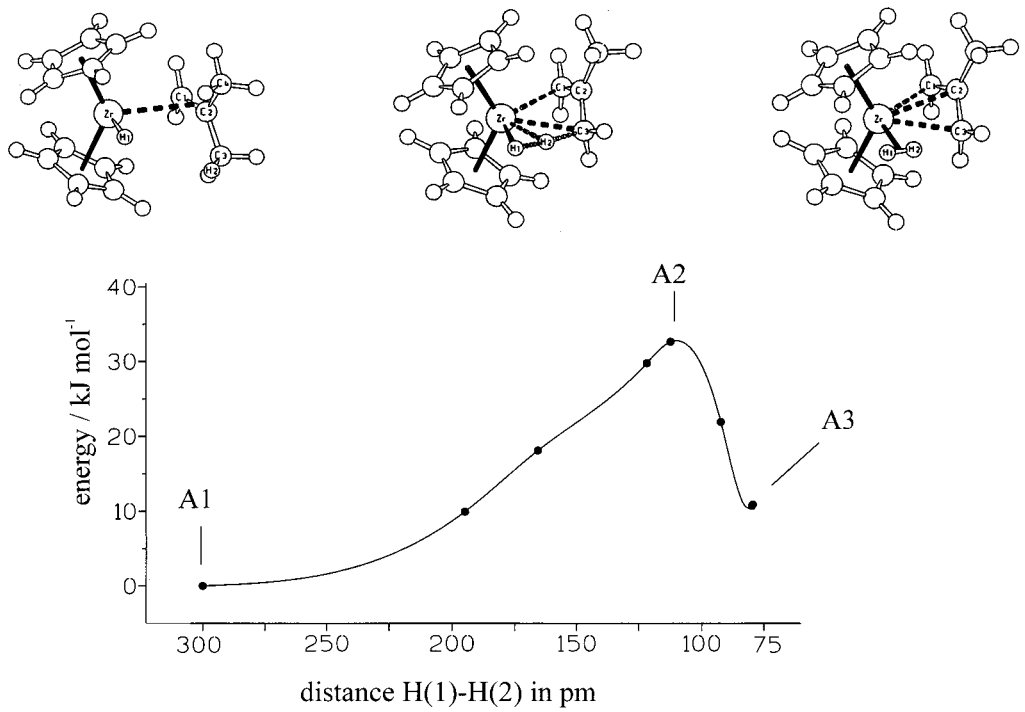

Figure 2. Energy profile and structures for the formation of a zirconium−allyl complex via C−H activation and subsequent dihydrogen formation.

Scheme 7

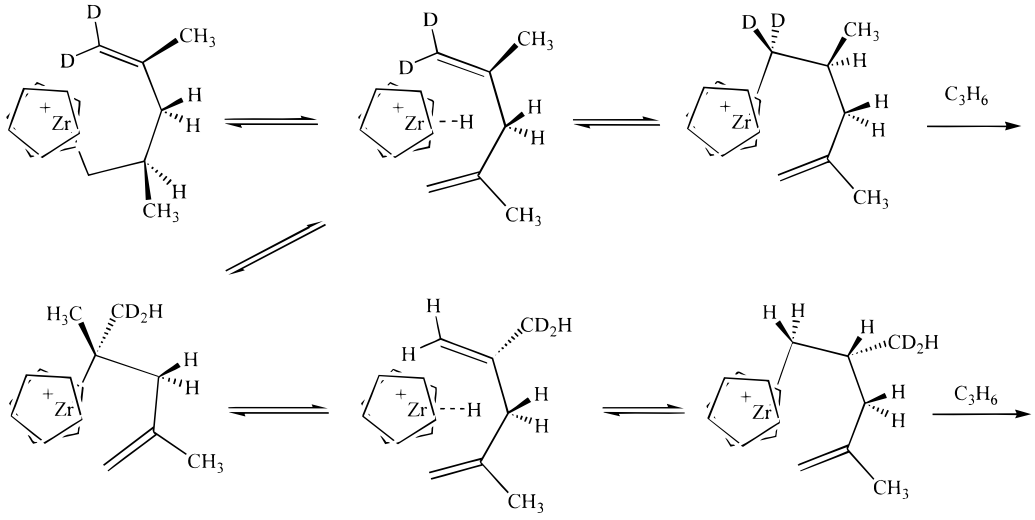

Computational Study

Experimental indication for formation of zirconocene allyl complexes and their reaction with propene raises the question as to reaction sequences and relative activation energies for these reactions in comparison to activation energies for chain growth and chain epimerization in homogeneous polymerization of propene with zirconocenes.

To gain more detailed insights into formation of a cationic zirconocene allyl complex during polymerization and further reaction of this cation with propene, these reactions were studied by density-functional methods. We investigated the reaction path in Scheme 2 for intramolecular C−H activation in the model system $[(C_5H_5)_2Zr-H(isobutene)]^+$ with special interest in activation energies for the formation of the dihydrogen ligand and its replacement by a propene molecule. To study the reaction of the resulting zirconocene allyl cation with propene, conceivable reaction paths for carbon−carbon bond formation were investigated by studying the insertion of a propene ligand into a Zr−σ-allyl or Zr−π-allyl bond.

4. Zirconium−Allyl Formation. As the initial state of the allyl formation reaction,[6,10] we chose the cation $[(C_5H_5)_2Zr-H(isobutene)]^+$, **A-1**. This cation can be formed, with a calculated activation energy of 40 kJ/mol,[17c] through β-hydrogen transfer to the metal from a Zr-bound isobutyl ligand, which represents a reasonable model for a Zr-bound polypropene chain. The energy of cation **A-1**, which is calculated to be 24 kJ/mol higher than the energy of the related isobutyl cation **A-0**,[17c] was set to 0 kJ/mol as the initial state of the allyl formation reaction.

Geometry optimization of the cation **A-1** revealed a

Downloaded by CARLI CONSORTIUM on June 29, 2009
Published on January 25, 2000 on http://pubs.acs.org | doi: 10.1021/om9906058

Downloaded by CARLI CONSORTIUM on June 29, 2009
Published on January 25, 2000 on http://pubs.acs.org | doi: 10.1021/om9906058

Table 2. Bond Distances and Angles for Geometries A-1 to A-3

	A-1	A-2	A-3
Zr−C(1)	255	256	245
Zr−C(2)	301	260	257
Zr−C(3)	364	254	254
Zr−H(1)	185	183	205
Zr−H(2)	372	196	206
Zr−CE[a]	216/216	220/218	219/217
CE−Zr−CE[a]	134	130	130
C−H(2)	111	136	203
H(1)−H(2)	293	112	84

[a] CE = C_5-ring centroid.

nearly C_s-symmetric conformation with Zr, H(1), C(1), and C(2) lying in the plane that bisects the angle between the C_5-ring ligand planes. The isobutene ligand is asymmetrically bound with Zr−C bond distances of 255 and 301 pm (Figure 2). Such asymmetrically bound olefin molecules were previously reported in related theoretical[17c,33] and single-crystal structural studies.[34] The hydride ligand H(1) is found at a distance of 185 pm from the Zr center: This is comparable with reported experimental and theoretical data of zirconocene hydride cations.[17c,33,35] Bond parameters calculated for cation **A-1** are listed in Table 2.

To model the intramolecular C−H activation, the distance between the hydride ligand H(1) and one hydrogen atom of an isobutyl methyl group, H(2), was chosen as reaction coordinate (Figure 2). Decreasing the H(1)−H(2) distance from 293 pm in **A-1** to 112 pm leads to the transition state **A-2** (Figure 2). Geometry optimization of cation **A-2** revealed a relatively low energy of 33 kJ/mol above **A-1** and bond distances and angles as listed in Table 2. The C(1)−C(2) bond vector is tilted out of the C_5H_5−Zr−C_5H_5 bisector plane by 24° such that one of the isobutene methyl groups (C(3)) appears in the equatorial plane within bonding distance to the metal center. The Zr−carbon bond distances (d(Zr−C(1)) = 256 pm and d(Zr−C(3)) = 254 pm) differ slightly from bond distances reported for a Zr-bound allyl ligand.[36] The C(3)−H(2) bond is elongated to a value of 136 pm; the Zr−H(2) distance of 196 pm for the bridging hydrogen ligand is longer than the terminal Zr−H(1) distance of 183 pm, which remains nearly unchanged in comparison to initial state **A-1**.

Further decrease of the H(1)−H(2) bond distance to approximately 80 pm leads to a minimum **A-3**, the cation $[(C_5H_5)_2$Zr-η^3-methallyl$(H_2)]^+$ (Figure 2). In this final state **A-3,** the methallyl ligand is bound in an η^3-fashion to the Zr center with bond distances of d(Zr−C(1)) = 245 pm and d(Zr−C(3)) = 254 pm, which are slightly shorter than those in transition state **A-2**. The geometry of the dihydrogen ligand shows a Zr−η^2-H_2 interaction with equal metal−hydrogen bond distances (d(Zr−H(1)) = 205 pm, d(Zr−H(2)) = 206 pm); both hydrogen atoms lie in the equatorial plane.

The energy of the final state, **A-3**, is calculated to be +11 kJ/mol above the initial state, **A-1**, and 22 kJ/mol below that of transition state **A-2**. In this cation **A-3** the dihydrogen ligand is weakly bound to the metal center by 25 kJ/mol and can be displaced by a propene molecule or an anion such as MAO−X^- or borate. Dissociation of the dihydrogen ligand requires about the same energy (25 kJ/mol) as the reverse reaction from cation **A-3** to **A-1** (22 kJ/mol). It is thus likely that a finite fraction of intermediate **A-3** will react under loss of dihydrogen especially in the presence of a large excess of monomer.

Formation of the cationic zirconocene allyl complex **A-3** from a cationic zirconocene alkyl resting state **A-0** requires an overall activation barrier of 67 kJ/mol and will thus normally be slow in comparison to chain growth (ca. 25−30 kJ/mol[37−42]). At sufficiently low olefin pressure, however, allyl formation could be competitive.

5. Insertion Pathways. Displacement of the dihydrogen ligand in cation $[(C_5H_5)_2$Zr-η^3-methallyl$(H_2)]^+$, **A-3**, by a propene molecule leads to intermediate **B-1** (Figure 3). The geometry optimization of $[(C_5H_5)_2$Zr-methallyl(propene)$]^+$ (**B-1**) reveals a loosely bound propene molecule and an η^3-methallyl ligand attached to the Zr center. The long Zr−propene bond distances of d(Zr−C(5)) = 441 pm and d(Zr−C(6)) = 420 pm are more indicative of an electrostatic interaction than of a propene ligand π-bound to the metal. The binding energy between the propene molecule and the $[(C_5H_5)_2$-Zr-methallyl$]^+$ fragment is calculated to be −28 kJ/mol, which is only 3 kJ/mol stronger than the bond energy of the dihydrogen ligand. The geometry parameters of the methallyl ligand (Table 3) remain unchanged compared to complex **A-3**.

To assess the activation barrier for insertion of propene into a Zr-bound allyl group in the cation **B-1**, we chose as the reaction coordinate the C(3)−C(5) distance between the inner olefin terminus (C(5)) and the inner methylene group of the allyl ligand (C(3)) (Figure 3, right), with all other geometry parameters allowed to relax.

The reaction profile calculated for optimized geometries along the reaction coordinate is shown in Figure 3. Decreasing the C(3)−C(5) bond distance from ca. 295 pm to 260 pm leads, over a shallow plateau, to the transition state **B-2** at a C(3)−C(5) bond distance of 226 pm (Figure 3). In the optimized geometry of the transition state **B-2** the metal−carbon bond distances of Zr−C(5) = 299 pm and Zr−C(6) = 239 pm are shorter than those in the initial state **B-1**. The methallyl ligand is asymmetrically bound to the metal with bond distances of d(Zr−C(1)) = 248 pm and d(Zr−C(3)) = 296 pm. The coordination site thus opened at the metal is occupied by the olefin ligand (Figure 3). The energy of transition state **B-2** is calculated to be 61 kJ/mol above that of the initial state **B-1**. Further decrease of the bond distance

(33) Margl, P.; Deng, L.; Ziegler, T. *Organometallics* **1998**, *17*, 933.
(34) Wu, Z.; Jordan, R. F.; Petersen, J. L. *J. Am. Chem. Soc.* **1995**, *117*, 5867.
(35) Yang, X.; Stern, C. L.; Marks, T. J. *Angew. Chem.* **1992**, *104*, 1406−1408.
(36) Wielstra, Y.; Duchateau, R.; Gambarotta, S.; Bensimon, C.; Gabe E. *J. Organomet. Chem.* **1991**, *418*, 183.
(37) Prosenc, M. H.; Schaper, F.; Brintzinger, H.-H. In *Metalorganic Catalysts for Synthesis and Polymerization*,; Kaminsky, W., Ed.; Springer-Verlag: Berlin, 1999; p 223.
(38) Margl, P.; Deng, L.; Ziegler, T. *J. Am. Chem. Soc.* **1998**, *120*, 5517.
(39) Støvneng, J. A.; Rytter, E. *J. Organomet. Chem.* **1996**, *519*, 277.
(40) Lohrenz, J. C. W.; Woo, T. K.; Ziegler, T. *J. Am. Chem. Soc*, **1995**, *117*, 12893.
(41) Yoshida, T.; Koga, N.; Morokuma, K. *Organometallics* **1995**, *14*, 746.
(42) Yoshida, T.; Koga, N.; Morokuma, K. *Organometallics* **1996**, *15*, 766.

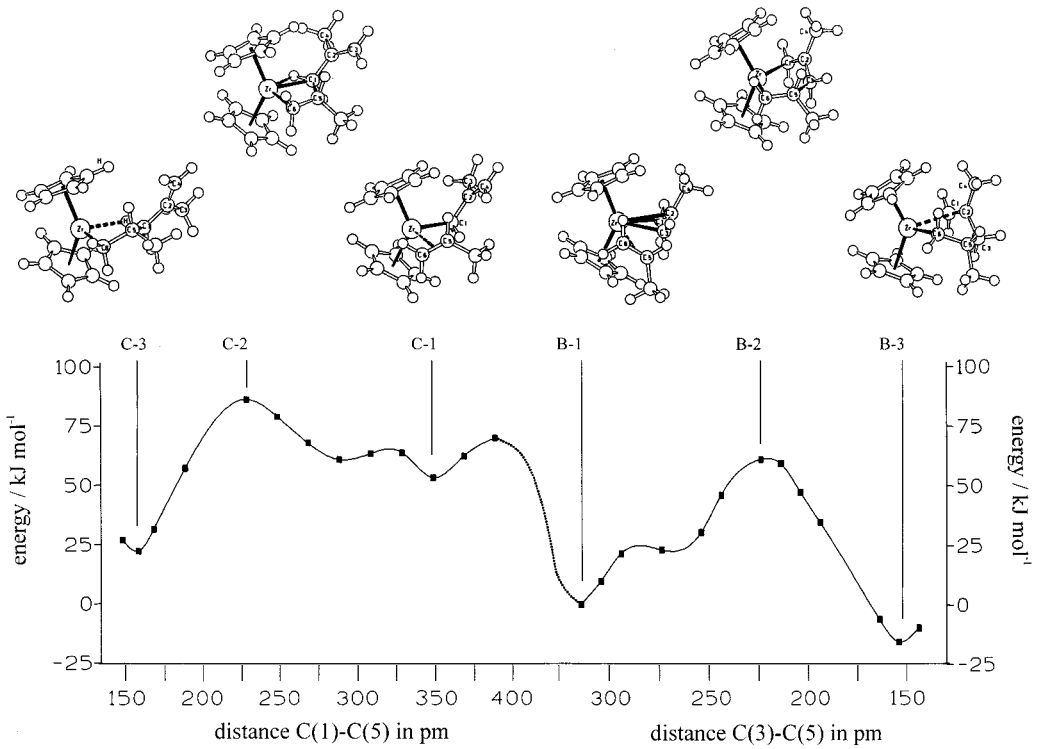

Figure 3. Energy profile and structures for the insertion of propene into a zirconium−allyl σ-bond (left) and into a zirconium−allyl π-bond (right).

Table 3. Bond Distances and Angles for Geometries B-1 to B-3

	B-1	B-2	B-3
Zr−C(1)	246	248	263
Zr−C(2)	259	261	303
Zr−C(3)	249	296	354
Zr−C(5)	441	299	346
Zr−C(6)	420	239	236
C(3)−C(5)	316	216	156
C(1)−C(2)	142	140	138
Zr−CE[a]	219/218	219/219	219/219
CE−Zr−CE[a]	133	131	134

[a] CE = C_5-ring centroid.

Table 4. Bond Distances and Angles for Geometries C-1 to C-3

	C-1	C-2	C-3
Zr−C(1)	223	331	296
Zr−C(2)	334		
Zr−C(3)			
Zr−C(5)	302	263	
Zr−C(6)	268	233	221
C(1)−C(5)	346	226	146
C(1)−C(2)	134	140	154
Zr−CE[a]	219/220	219/218	217/217
CE−Zr−CE[a]	130	134	135

[a] CE = C_5-ring centroid.

C(3)−C(5) leads to the final product **B-3** at a C(3)−C(5) bond distance of 156 pm. Geometry optimization of this cation **B-3** reveals the parameters listed in Table 3. The former propene ligand is now σ-bonded with its CH_2 terminus to the Zr center (d(Zr−C(6)) = 236 pm). The carbon atoms C(1) and C(2) of the allyl ligand form an olefin terminus (d(C(1)−C(2)) = 138 pm) and stabilize the unsaturated Zr center as shown by bond distances of d(Zr−C(1)) = 263 pm and d(Zr−C(2)) = 303 pm (Figure 3). The activation barrier for the process **B-1** to **B-3** is calculated to be 61 kJ/mol; it is thus ca. 35 kJ/mol higher than that for insertion of a propene ligand into a Zr−σ-ethyl bond in the cation $[(C_5H_5)_2$Zr-ethyl-(propene)$]^+$.[37,39,41,42]

An alternative reaction path involving insertion of a propene molecule into the Zr−C σ-bond of an η^1-bound allyl ligand was modeled by choosing the C(5)−C(1) bond distance as the reaction coordinate.

The optimized start geometry **C-1** (Figure 3, left) reveals that the η^1-bound methallyl ligand is rotated around its Zr−C(1) bond by 80°, with a Zr−C(1) distance of 223 pm. The geometry of cation **C-1** is similar to that expected for a σ-bound alkyl group in related cationic zirconocene complexes.[37−42] In this geometry, the substituents of the methallyl ligand and the olefin molecule point into an opening between the Zr-bound ligands to reduce nonbonding repulsion between substituents. The propene ligand is more strongly bound to the metal center in cation **C-1** than in cation **B-1** as indicated by shorter Zr−C(5) and Zr−C(6) bond distances (302 and 268 pm). The energy of species **C-1** is calculated to be 54 kJ/mol above that of cation **B-1**. This is close to the experimentally obtained activation energy for the exchange of *syn*- and *anti*-methylene protons of the allyl ligand, which involves a hapticity change similar to that described by the structural rearrangement from **B-1** to **C-1**.

The energy profile obtained from optimized geometries along the reaction path for the insertion of a propene ligand into the Zr−C(1) σ-bond is presented in Figure 3. Starting from cation **C-1**, a decrease of the Zr−C(1) bond distance leads over a plateau at 280 pm to transition state **C-2** at ca. 220 pm. The energy of this transition state **C-2** is calculated to be 32 kJ/mol above that of cation **C-1**, i.e., 86 kJ/mol above that of cation **B-1**. The geometry of transition state **C-2** shows a strong α-agostic interaction[29,42] with a Zr−H bond distance of

Downloaded by CARLI CONSORTIUM on June 29, 2009
Published on January 25, 2000 on http://pubs.acs.org | doi: 10.1021/om9906058

Downloaded by CARLI CONSORTIUM on June 29, 2009
Published on January 25, 2000 on http://pubs.acs.org | doi: 10.1021/om9906058

214 pm and a C(1)−H bond distance of 114 pm and is comparable to the geometries of transition states calculated for the insertion of an olefin into a Zr−alkyl σ-bond reported in the literature.[37−42] Further decrease of the C(1)−C(5) bond distance leads to final state **C-3**, the geometry of which shows a strong γ-agostic interaction. The energy of final state **C-3** is calculated to be 31 kJ/mol below that of initial state **C-1**. This final state **C-3** can rearrange—without any significant activation barrier—to final state **B-3** by replacing the γ-agostic interaction by coordination of the olefin carbon atoms (C(2),C(3)) to the metal center.

Overall activation barriers of +61 kJ/mol for insertion of a propene ligand into a Zr−η^3-methallyl bond represented by the sequence **B-1** → **B-2** → **B-3** and of +86 kJ/mol for insertion into a Zr−η^1-methallyl bond represented by the sequence **B-1** → **C-1** → **C-2** → **C-3** show that insertion into a Zr−allyl bond is possible and is more likely to take place into a Zr−allyl π-bond than into a Zr−allyl σ-bond. Rearrangement of the allyl group from initial state **B-1** to **C-1** is endothermic by 54 kJ/mol and thus disfavors insertion of a propene ligand into a Zr−methallyl σ-bond. Similar insertion mechanisms of olefins into π-allyl ligands were previously reported for insertion of butadiene into a Ni−allyl bond by Taube[44] and for ethylene insertion into Pd−allyl and Zr−allyl bonds.[12,45]

Conclusion

In conclusion, our results show that zirconocene−allyl species arising during olefin polymerization catalysis can be reactivated either by exchange with an aluminum alkyl cocatalyst or—in the presence of a borane activator—by olefin insertion into the Zr−allyl bond. Allyl−alkyl exchange with trimethyl aluminum or with MAO occurs, at moderate Al:Zr ratios, with rates on the order of ca. 0.1−1 s^{-1}, which are ca. 10−100 times slower than typical olefin insertions but comparable to the rates of chain transfer, e.g., to aluminum alkyls. Formation of transmetalation products with Al-bound methallyl end groups during polymerization catalysis would escape recognition since the final hydrolysis would convert them to normal 2-propenyl end groups.

Olefin insertion into a Zr−allyl species, which is recognizable by the appearance of internal unsaturation within the polymer chain,[14,15] must also be slower than olefin insertion into normal Zr−alkyl species by at least one order of magnitude, as shown by the observation that only a fraction of the borane-activated complex **2** reacts with added propene, which is then used up through multiple insertions into the ensuing Zr−oligomer units. DFT calculations illustrate that reactivation of a Zr-bound allyl ligand through insertion of a propene molecule requires a relatively high activation energy. Reactivation by insertion of propene is thus likely to be slower than that by reaction with dihydrogen, which regenerates a highly reactive zirconocene−olefin−hydride complex with an activation barrier of only ca. 20 kJ/mol. This provides an explanation for the increase of activity caused by addition of small amounts of dihydrogen to zirconocene-based polymerization systems.[46] In any case, formation of zirconocene−allyl species through one of the pathways represented in Schemes 1 and 2 is likely to cause serious reductions in catalyst acitivities by tying up substantial fractions of the catalyst.

Computational Methods

For geometry optimizations of the complexes studied, we used the gradient-corrected nonlocal density functional according to Becke[47] and Perdew[48] (BP). For all calculations the program DGAUSS (4.1)[49] with the medium integration grid option was used on a CRAY J916/6-1024. For the Zr atom we used an effective core potential base set with double-ζ quality in the valence region.[49] The DZVP[21] split valence basis set was used for all C and H atoms; for the J_{ij} Coulombic term[50] the A1[49] auxiliary basis was used for all atoms. All stationary points were checked by frequency calculations for the absence of negative eigenvalues and the presence of only one negative eigenvalue for each transition state.

Experimental Section

All reactions were performed under argon using Schlenk-line techniques or under nitrogen in a glovebox. Solvents were dried prior to use by refluxing over and distilling from sodium. Deuterated solvents were dried over 4 Å molecular sieves. $(C_5H_5)_2ZrClMe$,[19] $(C_5H_5)_2ZrMe_2$,[50] $(C_5H_5)_2Zr(C_4H_7)_2$,[20] $(CH_2C(CH_3)CD_2)MgBr$,[52] $B(C_6F_5)_3$,[53] Me_2Si(2-Me-4-^{t}Bu-$C_5H_2)_2ZrMe_2$,[54] Me_2Si(2-Me-indenyl)$_2ZrMe_2$,[54] $C_2Me_4(C_5H_4)_2ZrMe_2$,[54] $Me_2Si(C_5H_4)_2ZrMe_2$,[54] and $Ph_2C(C_5H_4)$(fluorenyl)$ZrMe_2$[54] were synthesized according to literature procedures. A 25% solution of MAO in toluene was donated by WITCO GmbH. $[PhNMe_2H][B(C_6F_5)_4]$ and $[Ph_3C][B(C_6F_5)_4]$ were obtained from BASF AG. All other chemicals were purchased from commercial suppliers and used without further purification.

^{1}H NMR spectra were recorded on Bruker AC 250 (250 MHz) or Bruker Avance 600 (600 MHz) instruments. ^{13}C NMR and ^{2}H NMR spectra were recorded on a Bruker Avance 600 (600 MHz) instrument. ^{19}F NMR spectra were recorded on a Bruker 400 (400 MHz) instrument. Polymer spectra were recorded on a Bruker AC 250 (250 MHz).

Synthesis and Characterization of Complexes $(C_5H_5)_2ZrMe(C_4H_7)$ (1). To a solution of $(C_5H_5)_2ZrMeCl$ (0.4 g, 2.3 mmol) in 15 mL of THF at 0 °C was added 5 mL of a solution of $(C_4H_7)MgCl$ in THF (c = 0.5 mol/L, 2.5 mmol). The mixture was allowed to warm to room temperature. After about 1 h the color of the solution had turned from pale yellow to orange. After stirring for another 2 h the solvent was

(43) Brookhart, M.; Green, M. L. H.; Wong, L.-L. *Prog. Inorg. Chem.* **1988**, *36*, 2.
(44) Tobisch, S.; Bogel, H.; Taube, R. *Organometallics* **1996**, *15*, 3563. Tobisch, S.; Bogel, H.; Taube, R. *Organometallics* **1998**, *17*, 1177.
(45) DiRenzo, G. M.; White, P. S.; Brookhart, M. *J. Am. Chem. Soc.* **1996**, *118*, 6225.
(46) Carvill, A.; Tritto, I.; Locatelli, P.; Sacchi, M. C. *Macromolecules* **1997**, *30*, 7056.
(47) Becke, A. *J. Chem. Phys.* **1986**, *84*, 4524. Becke, A. *J. Chem. Phys.* **1988**, *88*, 1053. Becke, A. *Phys. Rev.* **1988**, *A38*, 3098.
(48) Perdew, J. P. *Phys. Rev.* **1986**, *B33*, 8822. Perdew, J. P. *Phys. Rev.* **1986**, *B34*, 7406.
(49) Andzelm, J. W. *Density Functional Methods in Chemistry*; Labanowski, J. K., Andzelm, J. W., Eds.; Springer-Verlag: New York, 1991; p 155.
(50) Dunlap, B. I.; Connolly, J. W. D.; Sabin, J. R. *J. Chem. Phys.* **1979**, *71*, 3396.
(51) Samuel, E.; Rausch, M. D. *J. Am. Chem. Soc.* **1973**, *95*, 6263.
(52) Hill, E. A.; Boyd, W. A.; Desai, H.; Darki, A.; Bivens, L. *J. Organomet. Chem.* **1996**, *541*, 1.
(53) Pohlmann, J. L. W.; Brinckman, F. E.; Tesi, G.; Donadio, R. E. *Z. Naturforsch.* **1965**, *20b*, 1. Pohlmann, J. L. W.; Brinckman, F. E. *Z. Naturforsch.* **1965**, *20b*, 5.
(54) Beck, S.; Prosenc, M. H.; Brintzinger, H. H.; Goretzki, R.; Herfert, N.; Fink, G. *J. Mol. Catal. A: Chem.* **1996**, *111*, 67.

Downloaded by CARLI CONSORTIUM on June 29, 2009
Published on January 25, 2000 on http://pubs.acs.org | doi: 10.1021/om9906058

evaporated and the residue extracted with pentane. The pentane solution was reduced in volume in vacuo and cooled to −60 °C to yield 350 mg (53%) of $(C_5H_5)_2ZrMe(C_4H_7)$ (**1**) in the form of yellow needles.

^{1}H NMR (600 MHz, C_6D_6, 300 K): δ 5.29 (s, 10H, C_5H_5), 2.54 (s, 4H, $CH_2(CH_3)CCH_2$), 1.48 (s, 4H, $CH_2(CH_3)CCH_2$), −0.25 (br, 3H, $ZrCH_3$). ^{13}C NMR (62.5 MHz, C_6D_6, 300 K): δ 108.8 (C_5H_5), 67.92 ($CH_2(CH_3)CCH_2$), 30.2 ($ZrCH_3$), 27.2 ($CH_2(CH_3)CCH_2$).

^{1}H NMR (600 MHz, C_6D_5Br, 300 K): δ 5.47 (s, 10H, C_5H_5), 2.51 (s, 2H, $CH_2(CH_3)CCH_2$), 3.2 (s, 2H, $CH_2(CH_3)CCH_2$), 1.68 (s, 3H, $CH_2(CH_3)CCH_2$), 1.21 (br, 3H, $ZrCH_3$).

Anal. Found (Calcd): C, 61.56 (61.79); H, 7.18 (6.91).

$(C_5H_5)_2ZrMe(C_4H_5D_2)$ (3). To a solution of 200 mg (0.74 mmol) of $(C_5H_5)_2ZrMeCl$ in 10 mL of THF at 0 °C was added 3 mL of a solution of $(CH_2C(CH_3)CD_2)MgBr$ in THF (c = 0.25 mol/L). The mixture was allowed to warm to room temperature, during which the pale yellow solution turned orange. After stirring for 2 h the solvent was exchanged for pentane and the residue extracted three times. Partial removal of the solvent and storing at −60 °C afforded $(C_5H_5)_2ZrMe(C_4H_5D_2)$ (**3**) in the form of small orange needles. Yield: 150 mg (0.51 mmol, 70%).

^{2}H NMR (61.4 MHz, C_6H_6, 300 K): 2.42 (s, 2D). ^{1}H NMR (600 MHz, C_6D_6, 300 K): δ 5.29 (s, 10H, C_5H_5), 2.54 (s, 2H, $CH_2(CH_3)CCD_2$), 1.48 (s, 3H, $CH_2(CH_3)CCH_2$), −0.25 (br, 3H, $ZrCH_3$).

Reaction of $(C_5H_5)_2ZrMe(C_4H_7)$ (1) with Trimethylaluminum. Addition of 200 μL of a TMA solution (c = 1 mol/L) in C_6D_6 to 200 μL of complex **1** (c = 0.1 mol/L) resulted in an almost complete disappearance of the yellow color. New NMR signals that appeared in the reaction mixture in addition to those of TMA and **1** were assigned to $(C_5H_5)_2ZrMe_2$ and $(C_4H_7)Me_5Al_2$. Ratios of $(C_5H_5)_2ZrMe(C_4H_7)$ to $(C_5H_5)_2ZrMe_2$ as given in Table 1 were determined from the respective integrals of the C_5H_5 signals.

^{1}H NMR (600 MHz, C_6D_6, 300 K): δ_5.70 (s, 10H, $C_5H_5ZrMe_2$), 5.29 (s, 10H, $C_5H_5ZrMe(C_4H_7)$), 2.92 (br, 4H, $CH_2(CH_3)CCH_2AlMe_2$), 2.54 (s, 4H, $CH_2(CH_3)CCH_2$), 1.77(s, 3H, $CH_2(CH_3)CCH_2AlMe_2$), 1.48 (s, 3H, $CCH_2(CH_3)CCH_2$), −0.15 (s, 6H, $Cp_2Zr(CH_3)_2$), −0.25 (br, 3H, $Cp_2ZrCH_3(CH_2(CH_3)CCH_2)$), −0.42 (bbr, $AlMe_3$ and $CH_2(CH_3)CCH_2AlMe_2$). ^{13}C NMR (150 MHz, C_6D_6, 300 K): δ 110.3 ($C_5H_5ZrMe_2$), 108.8 ($C_5H_5ZrMe(C_4H_7)$), 51.5 ($CH_2(CH_3)CCH_2AlMe_2$), 67.9 ($CH_2(CH_3)CCH_2$), 28.2 ($CH_2(CH_3)CCH_2AlMe_2$), 27.2 ($CH_2(CH_3)CCH_2$), 30.2 (Cp_2ZrCH_3), −7.2 ($AlMe_3$ and $CH_2(CH_3)CCH_2AlMe_2$).

Reaction of $(C_5H_5)_2ZrMe(C_4H_7)$ (1) with $B(C_6F_5)_3$. Reaction of 300 μL of a 0.1 mol/L solution of **1** and 300 μL of a 0.11 mol/L solution of $B(C_6F_5)_3$ in C_6D_6 in an NMR tube at room temperature gave NMR signals that were assigned to complex $[(C_5H_5)_2Zr(C_4H_7)][MeB(C_6F_5)_3]$ (**2**) as outlined below. Formation of **2** was accompanied by precipitation of a red oil, which we were not able to isolate without decomposition. No precipitate occurred when orange complex **2** (0.05 mol/L) was generated by an analogous reaction in bromobenzene solution.

^{1}H NMR (600 MHz, C_6D_6, 300 K): δ 5.25 (s, 10H, C_5H_5), 2.45 (s, 4H, $CH_2(CH_3)CCH_2$), 1.4 (s, 3H, $CH_2(CH_3)CCH_2$), −0.3 (br, 3H, $CH_3B(C_6F_5)_3$). ^{19}F NMR (376 MHz, C_6D_6, 300 K): δ 132.1 (d, J_{F-F} 22 Hz, *o*-F), 163.8 (t, J_{F-F} 22 Hz, *p*-F), 166.4 (m, J_{F-F} 22 Hz, *m*-F).

^{1}H NMR (600 MHz, C_6D_5Br, 300 K): δ 5.47 (s, 10H, C_5H_5), 3.2 (s, 2H, $CH_2(CH_3)CCH_2$), 2.51 (s, 2H, $CH_2(CH_3)CCH_2$), 1.68 (s, 3H, $CH_2(CH_3)CCH_2$), 1.21 (br, 3H, $CH_3B(C_6F_5)_3$). ^{19}F NMR (376 MHz, C_6D_5Br, 300 K): δ −132.0 (d, J_{F-F} 22 Hz, *o*-F), −161.5 (t, J_{F-F} 22 Hz, *p*-F), −166.1 (m, J_{F-F} 22 Hz, *m*-F).

Reaction of $(C_5H_5)_2ZrMe(C_4H_5D_2)$ (3) with $B(C_6F_5)_3$. An analogous reaction of $(C_5H_5)_2ZrMe(C_4H_5D_2)$ with $B(C_6F_5)_3$ in bromobenzene gave signals assigned to complex $[(C_5H_5)_2Zr(C_4H_5D_2)][MeB(C_6F_5)_3]$ (**4**).

^{1}H NMR (600 MHz, C_6D_5Br, 300 K): δ 5.47 (s, 10H, C_5H_5), 3.2 (s, 1H, $CH_2(CH_3)CCD_2$), 2.51 (s, 1H, $CH_2(CH_3)CCD_2$), 1.68 (s, 3H, $CH_2(CH_3)CCD_2$), 1.21 (br, 3H, $CH_3B(C_6F_5)_3$). ^{19}F NMR (376 MHz, C_6D_5Br, 300 K): δ −132 (d, J_{F-F} 22 Hz, *o*-F), −161.5 (t, J_{F-F} 22 Hz, *p*-F), −166.1 (m, J_{F-F} 22 Hz, *m*-F). ^{2}H NMR (61.4 MHz, C_6H_5Cl, 300 K): 2.55 ($C_4H_5D_2$).

Reaction of $(C_5H_5)_2ZrMe(C_4H_7)$ (1) with *N*,*N*-Dimethylanilinium Perfluorotetraphenyl Borate. Reaction of equimolar amounts of $(C_5H_5)_2ZrMe(C_4H_7)$ (c = 2.5 mmol) and *N*,*N*-dimethylanilinium tetrakis(pentafluorophenyl)borate in bromobenzene at room temperature gave ^{1}H NMR signals that were assigned to $(C_5H_5)_2Zr(C_4H_7)^+$, $(C_5H_5)_2ZrMe^+$, *N*,*N*-dimethylaniline, isobutene, and methane in the following manner.

^{1}H NMR (250 MHz, C_6D_6, 300 K): 6.4 (t, J_{H-H} 7.5 Hz, *m*-H), 6.1 (t, J_{H-H} 7.5 Hz, *p*-H), 5.9 (d, J_{H-H} 7.5 Hz, *o*-H), 1.8 (coordinated aniline), 4.83, 4.75 $(C_5H_5)_2Zr(C_4H_7)^+$(*N*,*N*-dimethylaniline), 2.41 $(C_5H_5)_2Zr(CH_2C(CH_3)CH_2)^+$(*N*,*N*-dimethylaniline), 1.0 $(C_5H_5)_2Zr(CH_2C(CH_3)CH_2)^+$(*N*,*N*-dimethylaniline), 4.73 ($CH_2C(CH_3)_2$), 1.58 ($CH_2C(CH_3)_2$), 0.14 CH_4.

Reaction of $(C_5H_5)_2Zr(C_4H_7)_2$ with *N*,*N*-Dimethylanilinium Perfluorotetraphenyl Borate. Upon addition of 250 μL of borate solution (c = 10 mmol/L) to 250 μL of a solution of $(C_5H_5)_2Zr(C_4H_7)_2$ (c = 10 mmol/L) in bromobenzene, an instant color change from orange to pale yellow was observed, and ^{1}H NMR signals for isobutene, $(C_5H_5)_2Zr(C_4H_7)^+$(*N*,*N*-dimethylaniline), and free *N*,*N*-dimethylaniline (DMA) were detected in the reaction mixture.

^{1}H NMR (250 MHz, C_6D_6, 300 K): 6.4 (t, J_{H-H} 7.5 Hz, *m*-H), 6.1 (t, J_{H-H} 7.5 Hz, *p*-H), 5.9 (d, J_{H-H} 7.5 Hz, *o*-H), 1.8 (coordinated DMA), 4.83, 4.75 $(C_5H_5)_2Zr(C_4H_7)^+$(DMA), 2.41 $(C_5H_5)_2Zr(CH_2C(CH_3)CH_2)^+$(DMA), 1.0 $(C_5H_5)_2Zr(CH_2C(CH_3)CH_2)^+$ (DMA).

Reaction of $(C_5H_5)_2Zr(C_4H_7)_2$ with Trityl Perfluorotetraphenyl Borate. Reaction of equimolar amounts of $(C_5H_5)_2Zr(C_4H_7)_2$ and trityl tetrakis(pentafluorophenyl)borate in bromobenzene at 25 °C resulted in the appearance of several new signals in the (C_5H_5) region, isobutene, and a green discoloration, which indicates decomposition of the starting material. Variation of solvent, concentration, or temperature did not influence the reaction.

Reaction of $[(C_5H_5)_2Zr(C_4H_7)][MeB(C_6F_5)_3]$ (2) with Olefins. An NMR tube containing 0.5 mL of a 1 mM solution of **2** in toluene, prepared as described above, was cooled to −60 °C. At this temperature 1 equiv of olefin was added via a syringe. The resulting product was immediately measured starting from −60 °C to room temperature. ^{1}H NMR signals at 4.7−4.5 and 2.0−0.9 ppm in a ratio of approximately 1:15, assigned to short oligomers containing 4−5 monomer units, and the signals of the unreacted complex **2** were detected. Addition of a 50-fold excess of propene at room temperature gave oligomeric chains, with ^{1}H NMR signal integrals of the olefinic end group and those for the remainder of the polymer chain in a ratio of 1:80.

Polymerization of Propene and Ethene. A Schlenk vessel was charged with toluene (50 mL) and triisobutylaluminum (0.5 mol). The mixture was thermostated at 40 °C and saturated with the monomer to 1 bar. To start the polymerization, 5 mL of a 1 mM solution of **2** in toluene was added. The reaction was stopped after 30 min by adding an acidic methanol solution. The resulting solution was washed with $NaHCO_3$ solution and water, and the organic layer was separated and dried with Na_2SO_4. Evaporation of the solvent in vacuo gave an oil, which is soluble in $C_2D_2Cl_4$ at room temperature.

Reaction of $(C_5H_5)_2ZrMe(C_4H_5D_2)$ (3) with $B(C_6F_5)_3$ and Propene. In an NMR tube 250 μL of a solution of **3** (0.025 mmol) in chlorobenzene was combined with 250 μL of a solution of tris(pentafluorophenyl)borane (0.03 mmol) at room temperature. To the resulting ion pair $[(C_5H_5)_2Zr(C_4H_5D_2)]$-

$[MeB(C_6F_5)_3]$ (**4**) was added 10 equiv of propene, and ^2H NMR spectra were recorded (cf. Figure 1). In another experiment, 10−12 equiv of propene was added to the ion pair **4**; after 5−10 s the reaction mixture was quenched by adding 5 μL of H_2O, and ^{13}C and ^2H NMR spectra were recorded. In this case the ratio of terminal $D_2C{=}C$ to the sum of the other D signals was 1:20.

Acknowledgment. Helpful discussions with Professor Ulrich Steiner, University of Konstanz, the recording of ^2H and two-dimensional spectra by Dr. Armin Geyer and Anke Friemel, and allocation of computing time by the Computing Center of the University of Konstanz are gratefully acknowledged. We thank Witco GmbH for the donation of MAO solutions. Financial support of this work was provided by BASF AG, Bundesministerium für Forschung und Technologie, and by funds of the University of Konstanz.

Supporting Information Available: Equations used for the determination of exchange equilibrium constant K_{ex} and of rate constants k_{ex} for methyl/methallyl exchange and data on the temperature dependence of k_{ex} are available free of charge via the Internet at http://pubs.acs.org.

OM9906058

Downloaded by CARLI CONSORTIUM on June 29, 2009
Published on January 25, 2000 on http://pubs.acs.org | doi: 10.1021/om9906058